Effect of carbon content and annealing atmosphere on phase purity and morphology of Li_2MnSiO_4 synthesized by a PVA assisted Sol-Gel method

Nils Wagner[a], Ann-Mari Svensson[a] and Fride Vullum-Bruer[a]

[a]*Department of Materials Science and Engineering, Norwegian University of Science and Technology,*

7491 Trondheim, Norway

Abstract

Lithium transition metal orthosilicates of the general formula Li_2MSiO_4 have gained great interest as potential positive electrode material for Li-ion batteries. This study reports the dependence of phase purity and morphology on heat treatment atmosphere and the amount of corn-starch as carbonization agent during a PVA assisted sol-gel synthesis of nano-sized porous Li_2MnSiO_4/C composites. All samples were indexed to the orthorhombic $Pmn2_1$ polymorph, but samples with carbon contents less than 6 % showed traces of the second orthorhombic polymorph Pmnb. Highest phase purities and a desired porous nano-sized morphology were obtained when heat treatments were carried out in 5 % H_2 and corn-starch amounts were $\geq$ 25 wt. %. Powders with varying carbon amounts were produced and the electrochemical performance was determined by galvanostatic cycling at different current densities. Samples with a corn-starch amount of 25 wt. % offered the highest initial discharge capacity of 155 $mAhg^{-1}$ at a current density of 3 mAg^{-1}.

1 Introduction

Since the discovery of $LiFePO_4$ as a cathode material for Li-ion batteries by Padhi *et al.* in 1997 [1] polyanion based materials gained great attention as potential Li-ion battery cathodes. Furthermore, polyanion based materials also reveal materials which in theory allow Li extraction/insertion beyond one Li ion per formula unit. Orthosilicates with the general formula Li_2MSiO_4 (M = Mn, Fe, Co) could in principle deliver two Li ions per formula unit, giving theoretical capacities up to 333 $mAhg^{-1}$. This is assuming that the transition metal possesses two redox couples within the potential window of a Li-ion battery and that the structure does not collapse [2, 3]. Dominko *et al.* first reported on the synthesis of Li_2MnSiO_4, later called LMS as a promising candidate for Li-ion cathode materials [4]. LMS can in theory extract/insert beyond 1 Li per formula unit since manganese can undergo reversible redox reactions between +2 and +4. A challenge is the structural instability during cycling, which might be caused by a Jahn-Teller distortion of the tetrahedrally coordinated Ar $3d^4$ ion Mn^{3+} [5]. This might be eliminated by nano-structuring or implementing stabilizing dopants. However, in order to apply adequate doping strategies the synthesis of the mother compound LMS must be optimized with regard to a desired morphology and a minimum of parasitic secondary phases. Moreover, a general drawback of the orthosilicates is the rather low electronic and Li ionic conductivities. Electronic conductivity values reported in literature are about 3×10^{-14} Scm^{-1} at 60 °C [6]. This very poor conductivity value, which at room temperature is even about two orders of magnitude lower, needs to be overcome by applying a conductive coating (e.g. carbon). At the same time the particle size must be reduced to limit the mean diffusion length for Li ions [6,7].

The synthesis and properties of LMS was recently reported by different synthesis methods. Values in brackets give the initial discharge capacity reported and the according reference: A solution route (210 $mAhg^{-1}$ [8]), the Pechini method (185 $mAhg^{-1}$ [9], 110 $mAhg^{-1}$ [10], 147 $mAhg^{-1}$ [11]), sol-gel (181.6 $mAhg^{-1}$ [12], ~190 $mAhg^{-1}$ [13]), polyol method (132 $mAhg^{-1}$ [14]), solid state synthesis (160 $mAhg^{-1}$ [15]) and molten carbonate synthesis (156 $mAhg^{-1}$ [16]). Reported Pechini sol-gel syntheses are based on acetate precursors which react as buffer in a pH range of 4-5 which is unfavorable for the hydrolysis of TEOS. Furthermore, they take a long time, up to 8 days including an ageing step and use technical polymers such as poly-N-vinylamide [9, 10, 11]. Also other technical substances such as lactones and phenolic resins are used as carbon sources [12, 13].

Here we report on a simple wet chemical approach, namely an acidic PVA assisted sol-gel method using metal nitrates and TEOS as silicon precursor with subsequent carbothermal reduction using simple corn-starch and an Ar/H_2 atmosphere as reducing agents. The rather quick synthesis yields nano-sized LMS particles with high phase purity, aggregated in a porous manner. Residues of PVA and the introduced corn-starch which was incorporated in amounts from 0 to 50 wt. %, provide a carbon coating on the LMS particles (LMS/C composite) and thus enhance the electronic conductivity. In contrast to many other studies the secondary phases were not only indexed but quantified in order to gain information about the influence of atmosphere and carbonizing agent on the phase purity of LMS.

2 Experimental

2.1 Material synthesis

The acidic, PVA assisted Li_2MnSiO_4 sol-gel synthesis described in this work is based on a Li_2FeSiO_4 sol-gel process reported by Zhou *et al.* [17]. with optimized parameters for LMS. 0.03 mole $Mn(NO_3)_2$ * 4 H_2O (Merck Ensure for analysis, > 98 %) and 0.06 mol dried $LiNO_3$ (Alfa Aesar, 99 %) were dissolved in 25 mL deionized H_2O and the pH was set to ~1.5 by adding HNO_3 (Sigma Aldrich ≥ 65 % pro Analysi). 0.03 mol tetraethyl orthosilicate (TEOS) (VWR 99 %) were dissolved in 20 mL EtOH and added to the Li-Mn solution under vigorous stirring. The pale pink solution was stirred for 20 min at room temperature, before 1.14 g PVA (Sigma Aldrich Mowiol 10-98, M_w = 61000) dissolved in 20 mL was added. The pH of the solution was ~2.5. To ensure complexing of the metal cations, the solution was stirred for 1 h in a closed beaker at 60 °C, and then evaporated at 60 °C for 6 h until gelation occurred.

The formed gel was aged for 72 h in a closed Ar filled beaker before it was dried for 4 h at 130 °C. The dried gel was ground and calcined for 1 h at 450 °C in air or in 95 % Ar 5 % H_2 later called H-Ar-mix-5 to combust the nitrates and parts of the organic residues. After the calcination the LMS precursor was mixed with different amounts of corn-starch (Carl Roth GmbH & Co. KG for laboratory use) (0-50 wt. %) as carbon source. An EtOH based suspension of the LMS precursor and corn-starch was intensively mortared till dryness. The final heat treatment for 10 h at 700 °C was performed in Ar or H-Ar-mix-5. A flow chart summarizing the synthesis with optimize parameters is shown in Fig. 1.

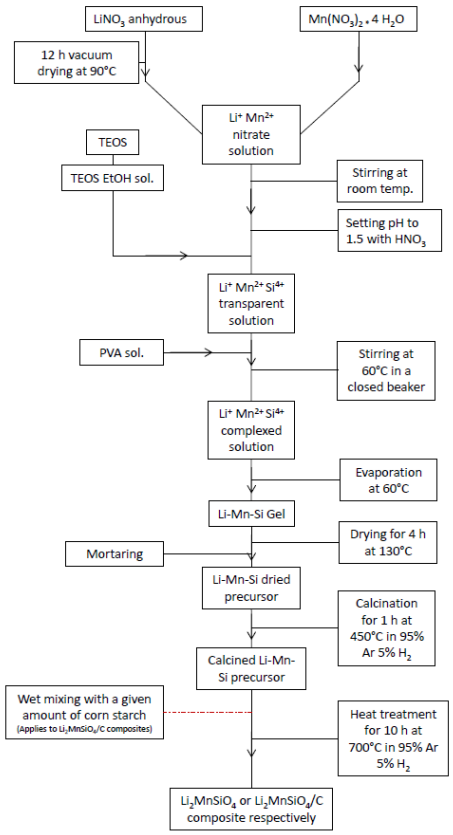

Fig 1: Summarizing flow chart with optimized parameters for the LMS and LMS/C synthesis

2.2 Characterization

Powder X-ray diffraction patterns were recorded on a Bruker D 8 Advance Da-Vinci with a LynxEye Xe detector working in Bragg–Brentano (Θ/2Θ) geometry. Patterns were recorded using CuK_α and MoK_α radiation from 2Θ = 15–75° and 5-75°, respectively. Lattice parameter calculations, full pattern refinements and quantifications of secondary phases of powder X-ray diffraction patterns recorded using MoK_α radiation were done with the software Topas (Bruker AXS Version 4.2). The peak shape was refined using a Pseudo-Voigt approximation (PV2). The

atomic positions not fixed by the geometry of the space-group $Pmn2_1$ were allowed to converge, starting with the heaviest element. Refined parameters were used to quantify the phase fraction of powder diffraction patterns recorded using CuK_α radiation. Here, a fundamental parameter approach was used to fit the peak shape.

Surface area and porosity data were measured by nitrogen adsorption on a Micrometrics Tristar 3000. Powders were dried at 250 °C for 12 h in vacuum prior to analysis. A total of 94 points were measured for the adsorption/desorption isotherms.

The carbon content was determined with an Eltra CS 800 elementary analyzer. Morphology investigations were carried out by transmission electron microscopy. TEM analysis was done on a double C_s corrected cold field emission gun JEOL JEM-ARM200F operated at 200 kV, equipped with a large solid angle Centurio SDD (Silicon Drift Detector). For microscopy investigations, the powders were dispersed in isopropanol and sonicated for 20 min. A small droplet of the powder/alcohol suspension was placed on an amorphous carbon coated Cu TEM grid.

Assessment of electrochemical properties was done by galvanostatic charge-discharge measurements between 1.5 and 4.5 V and 1.5 and 4.8 V at 24 °C using a Maccor 4200. CR2016 coin cells were assembled in a glove box (dry Ar atmosphere) using LMS or LMS/C as cathode, Li-foil as anode and a Celgard 2400 film as electrode separator. The electrolyte consisted of 1 M $LiPF_6$ (Aldrich ≥ 99.99 %) dissolved in a 3:7 volume ratio of ethylene carbonate (Sigma 99 %) and diethyl carbonate (Aldrich ≥99 %). For cathode fabrication, the active material, LMS or LMS/C respectively was mixed with 10 wt. % conductive carbon (Super P) and 5 wt. % PVDF (Kynar, reagent grade) as binder. N-Methyl-2-pyrrolidone (NMP) (Sigma Aldrich > 99 %) was added as solvent and a slurry was formed by ball milling on a RETSCH mixer mill in a stainless

steel container. The slurry was tape casted on Al foil as current collector and dried for 12 h at 90 °C in a vacuum oven. Cast thicknesses were about 15-20 µm. Capacities are reported with respect to the mass of LMS or the LMS/C composite. The charge rate C was defined as a current density of 330 mAg^{-1} = 1C.

3 Results and discussion

3.1 Influences of the atmosphere and corn-starch amount on the phase purity

All obtained dried gels were amorphous but showed minor $LiNO_3$ precipitates in the XRD patterns which are shown in the supporting material. The weight loss during calcination in H-Ar-mix-5 and in air was measured to be approximately 37 wt. %.The phase purity of the resulting LMS/C showed a strong dependence on the p_{O_2} during the heat treatments which is dependent on the gas composition and the corn-starch content. Best results were achieved when both heat treatments were carried out in H-Ar-mix-5 and initial corn-starch contents were ≥ 25 wt. %. LMS adopts Li_3PO_4 structures and is reported to exist in two orthorhombic and two monoclinic polymorphs, namely $Pmn2_1$, Pmnb, $P2_1/n$ and Pn [4, 18, 19, 20]. All samples were indexed to the orthorhombic $Pmn2_1$ polymorph of LMS. Secondary phases present for LMS and LMS/C with low carbon content were Li_2SiO_3, Mn_2SiO_4 and MnO, LMS/C samples produced with corn-starch amounts of ≥ 25wt. % showed minor Li_2SiO_3 and MnO impurities. The different heat treatment parameters and corn-starch content of a sample series A-D are given in table 1.

Table 1: Heat treatment atmospheres and carbon source amount of samples A-D

Sample	Calcination atmosphere	Corn-starch [wt. %]	Heat treatment atmosphere
A	Air	30	Ar
B	Air	25	H-Ar-mix-5
C	H-Ar-mix-5	25	Ar
D	H-Ar-mix-5	25	H-Ar-mix-5

Fig. 2a shows the phase composition of the corresponding samples. It can be seen in the next section that 30 wt. % corn-starch in powder A yields a similar carbon content in the final powder as 25 wt. % in powder D. Although the error of theses quantifications might be as large as 5 %, clear trends in increased phase purity are observed. Furthermore, quantified data of sample D using MoK_{α} and CuK_{α} radiation is in agreement, which indicates the accuracy of the values. Calcination in H-Ar-mix-5 is believed to hinder parasitic Mn oxidation and the formation of multivalent Mn oxides that need to be reduced during the final heat treatment. XRD patterns of the calcined precursors showed some crystalinity but were mainly amorphous and are shown in the supporting material. Fig 2b shows the phase fraction with regard to the added corn-starch content from 0 to 50 wt. % for powder samples where both heat treatments were carried out in H-Ar-mix-5. It has to be mentioned that the shown phase fractions refer to the crystalline part of the samples and disregard the amorphous carbon content. Samples containing 10 and 20 wt. % corn-starch were not synthesized and the quantification of a sample containing 5 wt. % corn-starch was disregarded due to an unidentified secondary phase. The phase purity of all samples with added corn-starch amounts of 25 wt. % and more is higher than 95 wt. %. The difference in phase fraction of samples with added corn-starch amount $\geq$ 25 wt. % is well within the error range of Rietveld based quantifications. In addition, an increase in the amorphous carbon content caused by addition of more corn-starch in the synthesis will reduce the signal to noise ratio, thus

it cannot be concluded if there is a significant difference in phase purity for corn-starch amounts of 25 wt. % or higher. Samples containing less corn starch showed lower phase purities and the appearance of a second orthorhombic LMS polymorph (Pmnb). This polymorph shows a 2Θ diffraction peak at about 30.6 ° under CuKα radiation which is often disregarded or confused with a Mn_2SiO_4 secondary phase which shows a peak at 31.2 ° 2Θ. As a result, significant amounts of Pmnb phases may be present in samples claimed to be indexed to $Pmn2_1$ [11,13,15]. Powder XRD patterns of samples calcined and reduced in H-Ar-mix-5 with varying corn-starch content are given in Fig. 3. The calculated carbon content is based on carbon content measurements shown in the following chapter. Part b shows a full pattern refinement using MoK_α radiation, the corresponding lattice parameters for the orthorhombic $Pmn2_1$ unit cell were a = 6.3062 Å, b = 5.3844 Å and c = 4.9656 Å and are in agreement with data from literature [4]. All further presented results are based on LMS and LMS/C powders synthesized with optimized parameters where both heat treatments were carried out in H-Ar-mix-5.

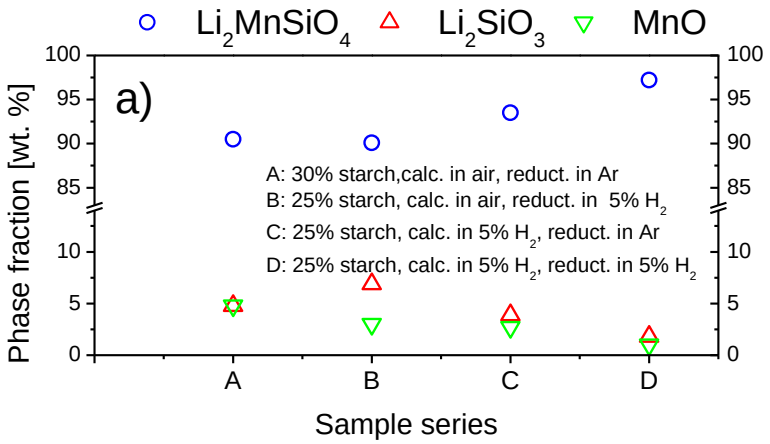

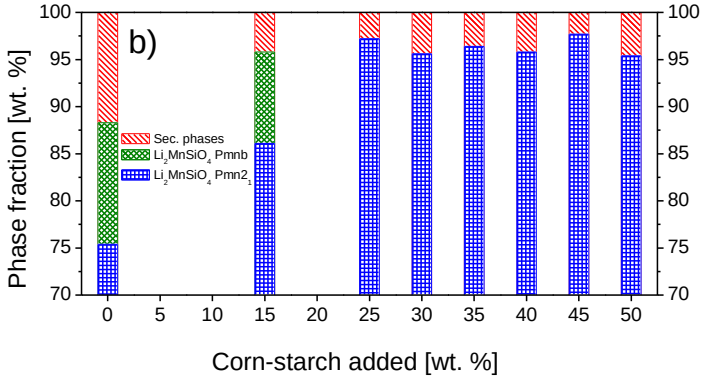

178

179

180 **Fig. 2: a) Phase composition for different heat treatment atmospheres. b) Phase fraction for**

181 **different starch contents at optimized synthesis parameters**

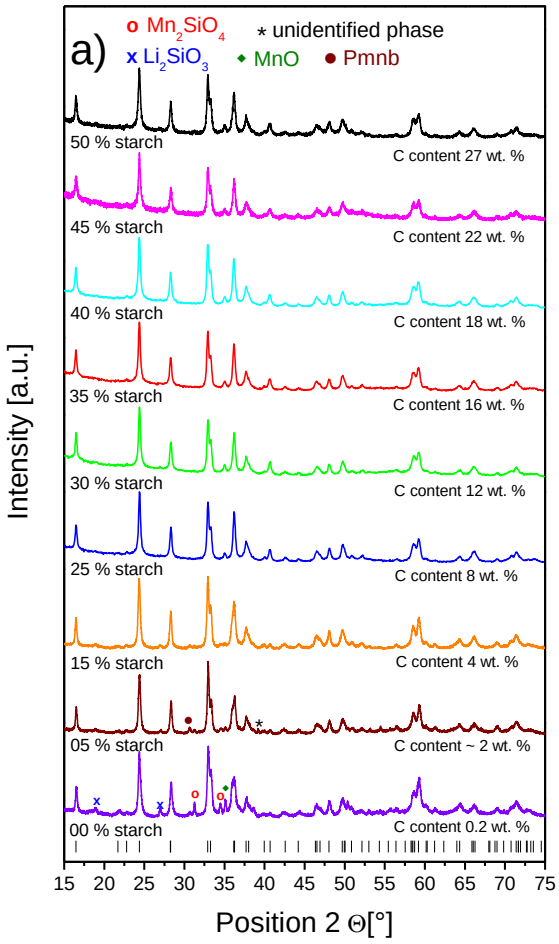
a)
o Mn2SiO4
x Li2SiO3
* unidentified phase
◆ MnO
● Pmnb
50 % starch
C content 27 wt. %
45 % starch
C content 22 wt. %
40 % starch
C content 18 wt. %
35 % starch
C content 16 wt. %
30 % starch
C content 12 wt. %
25 % starch
C content 8 wt. %
15 % starch
C content 4 wt. %
05 % starch
C content ~ 2 wt. %
00 % starch
C content 0.2 wt. %
Intensity [a.u.]
15 20 25 30 35 40 45 50 55 60 65 70 75
Position 2 Θ[°]

182

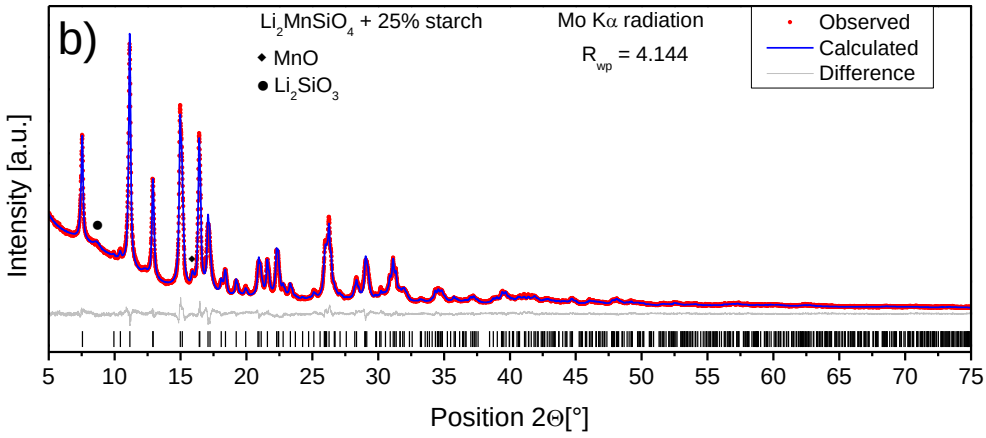
b)
Li2MnSiO4 + 25% starch
◆ MnO
● Li2SiO3
Mo Kα radiation
Rwp = 4.144
Observed
Calculated
Difference
Intensity [a.u.]
5 10 15 20 25 30 35 40 45 50 55 60 65 70 75
Position 2Θ[°]

183

Fig 3: a) Powder XRD pattern (CuK$_\alpha$ radiation) of LMS/C synthesized with optimized parameters and different corn-starch contents. Residual carbon content is given. Asterisk marks the unidentified secondary phase in the 5% sample. b) Full pattern refinement (MoK$_\alpha$ radiation) of a LMS/C sample

3.2 Morphology and carbon content

The PVA assisted sol-gel synthesis with additional gel ageing was performed to obtain a strong gel network which does not collapse and yield porous nano-structured materials with high surface areas. Hydroxyl groups of the PVA can, in addition to bridging to polymerized silanol groups of the network, complex the metal cations and thus strengthen the network. It was shown for Li_2FeSiO_4, a very similar compound, that the addition of a complexing/bridging agent (PVA) during a sol gel method is essential to obtain a nano-porous structure [21]. The ageing for 72 h under Ar atmosphere was performed in order to gain further structural strength by syneresis and further bond formation. The aged gel can withstand the capillary forces during drying and keep a porous structure [17]. Ar atmosphere was applied to hinder parasitic reactions between the expelling liquid and oxygen from the atmosphere.

The initial corn-starch content showed a strong influence on the resulting morphology of the powder. The residual carbon content of LMS/C composites with varying amounts of corn-starch (heat treated in H-Ar-mix-5) was measured with an elementary analyzer. Also three different LMS/C samples heat treated in Ar were measured. The results are shown in Fig. 4. An exponential growth fit for the samples heat treated in H-Ar-mix-5 is added as a guide for the eye.

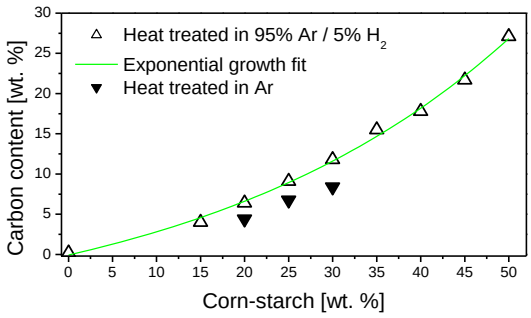

207

208

209 **Fig 4: Carbon content of LMS/C samples heat treated in H-Ar-mix-5 and in Ar respectively**

210

211 Fig. 5a shows the surface area divided into micropore area and external area according to T-plot
212 theory [22, 23] for powders with the corresponding isotherms in the insert. The sum of
213 micropore area and external area is equal to the BET surface area. In this case, the presentation
214 of just the BET surface area without further differentiation would be inconvenient, since
215 micropores are by definition smaller than 2 nm and thus inaccessible to complexed Li ions [17].
216 Here the external area is the surface area that is not attributed to micropores. By dividing the
217 surface area in micropore area and external area the accessible surface area can be defined. This
218 gives a more meaningful presentation of a porous electrode surface area. The powder
219 morphology for corn-starch contents $\geq$ 25 wt. % consists out of porously agglomerated particles
220 with a particle size of about 40-50 nm, while powders containing lower amounts of corn-starch
221 showed a much lower surface area. It is believed that the carbon layer formed on the particle
222 surface hinders particle growth to a certain extent. Since powders containing a relatively low
223 amount of carbon are not covered by this film they might show a higher degree of particle
224 growth and thus a reduced surface area. A high amount of meso/macro-porosity, which is

accessible for complexed Li ions, is present. In addition, the powders show an increasing amount of micro-porosity with increasing corn-starch amount. This micro-porosity is believed to be attributed to the porous nature of the amorphous carbon layer on the particle surface. Fig 5b shows the pore distribution based on desorption data according to BJH theory [24], of different corn-starch contents between 2 and 100 nm with a highlighted area between 3-6 nm. This area shows a peak in porosity increasing with increasing corn-starch amount, thus it can as well be attributed to the carbon layer. TEM analysis (Fig 6.) revealed the porous nature of the agglomerated nano-particles. Furthermore, Fig 6b and c show the carbon coated particle surface of a sample containing 25 and 50 wt. % corn-starch, respectively. The porosity of this layer is clearly visible in Fig 6c so it is concluded that the increasing micro-pore area and the abnormal porosity between 3-6 nm corresponds to the carbon layer. The electron diffraction pattern of LMS is shown in Fig 6d. The main diffraction lines of polycrystalline $Pmn2_1$ LMS are visible. Comparing Fig. 6a and 6c also reveals the effect of the carbon source on the particle size. Whilst crystallites in Fig. 6a, where 25 wt. % corn-starch was added to the synthesis, show particle sizes from approximately 50 to 100 nm, crystallites of the powder containing 50 wt. % corn-starch are in the range of 20-40 nm, which can be seen in Fig. 6c.

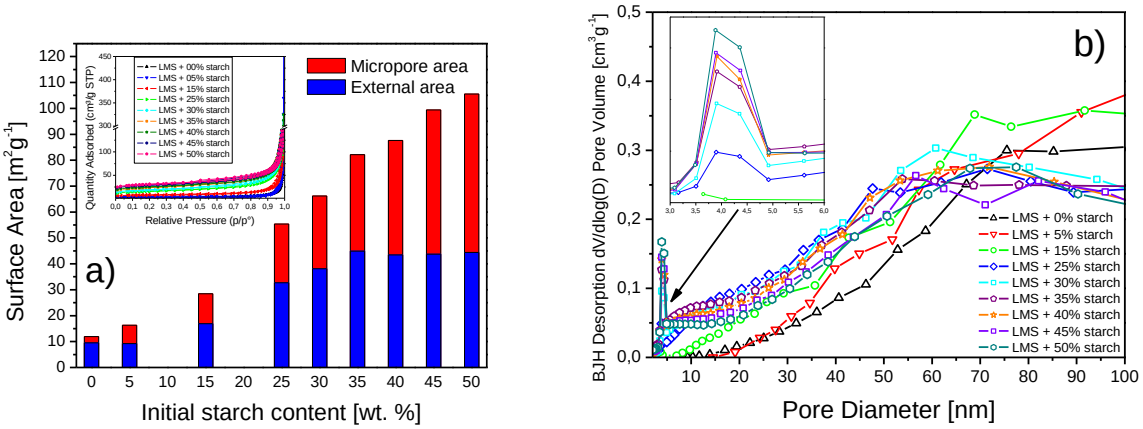

Fig. 5: a) BET surface area for powders with varying corn-starch content, including isotherms and micro-pore/external area separation. b) Pore size distribution for powders with varying corn-starch content

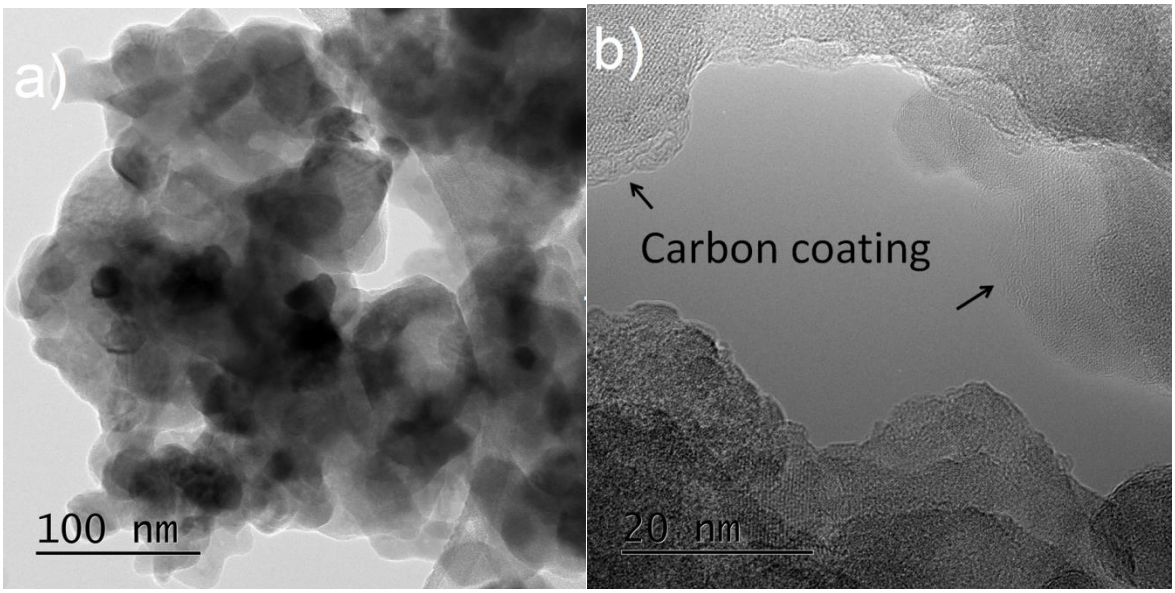

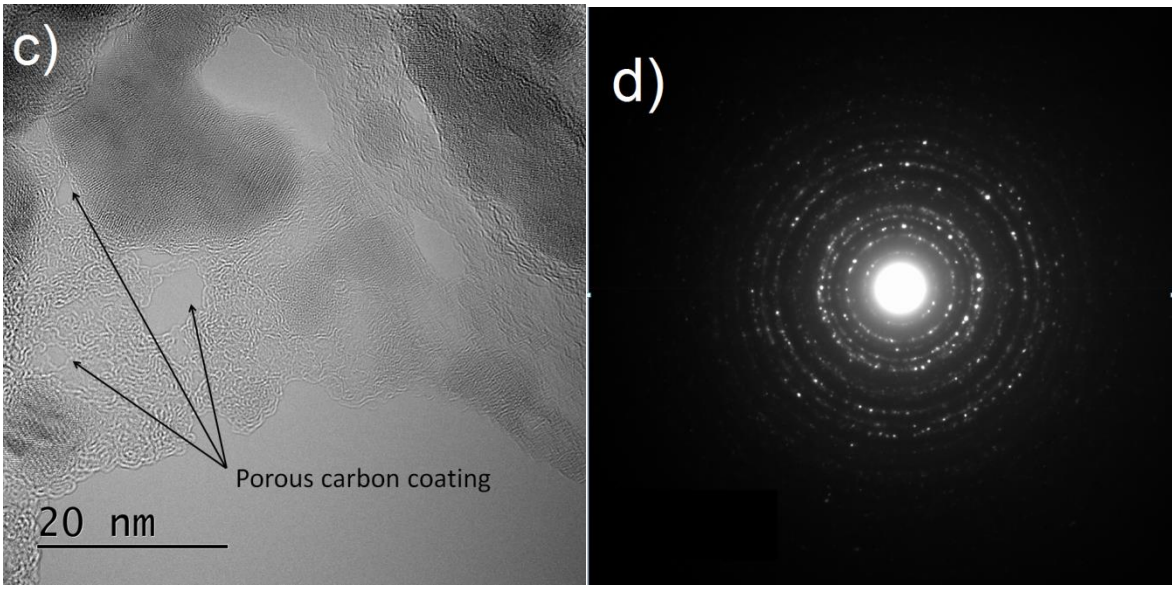

Fig. 6: TEM micrographs of A) the agglomerate structure of a sample containing 25 wt. % corn-starch, B) the carbon coating of a sample containing 25 wt. % corn-starch, C) the porosity of the carbon coating of a sample containing 50 wt. % corn-starch and D) the electron diffraction pattern

3.3 Electrochemical characterization

To investigate the importance of the carbon content and hence the electronic conductivity, CR2016 coin cells were fabricated with LMS cathodes produced using 0, 5, 15, 25, 35, 45 and 50 wt. % added corn-starch. Furthermore, the cathode contained 10 wt. % Super P conductive carbon and 5 wt. % PVDF as binder. The counter electrode was in all cases Li foil. These coin cells were galvanostatically cycled between 1.5 and 4.5 V at charge rates corresponding to C/33 and C/4. Fig.7 shows the first two cycles of the corresponding coin cells and the reversible

discharge capacity for 15 cycles where the charge rate was C/33 in the first five cycles C/4 for the following 5 cycles and C/33 for the last five cycles.

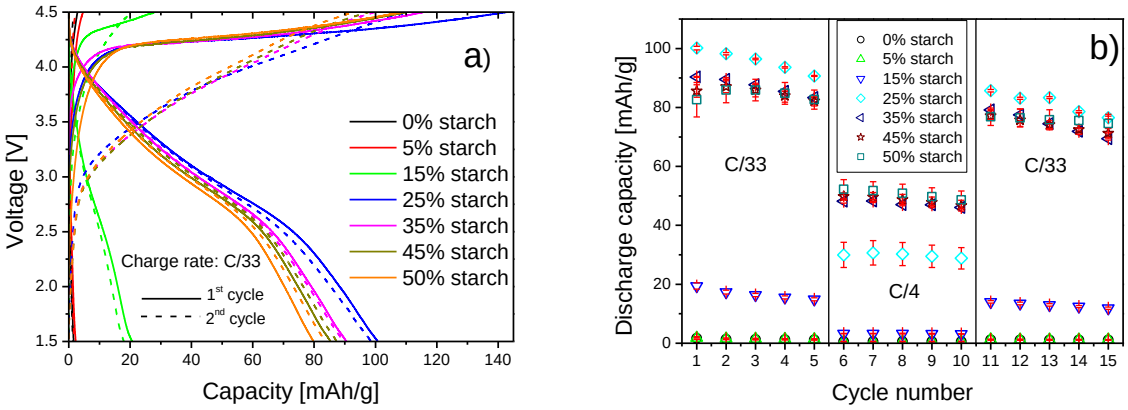

Fig. 7: Galvanostatic cycling of LMS cathodes offering a varying amount of corn-starch as carbon source. a) First two cycles at C/33. b) Reversible discharge capacity for 15 cycles at different charge rates

All samples showed an irreversible capacity loss of 20-30 % during the first cycle. The oxidation of the electrolyte is expected to contribute to a fraction of this loss, but cannot solely be responsible for the irreversible capacity loss. It is therefore likely that the extraction of Li ions is partly irreversible. Furthermore, Molenda *et al.* observed structural changes in the carbon coating by XPS which could also contribute to the irreversible capacity loss by a loss in electronic conductivity [12].

The need of a conductive coating is clearly seen. LMS cathodes with no carbon or only 5 wt. % addition of corn-starch showed very low reversible capacities of about 1.5-2 $mAhg^{-1}$ in the first cycle. 15 wt. % corn-starch which corresponds to 4 wt. % residual carbon is still not sufficient to

obtain the necessary coating. The peak in performance was observed with and addition of 25 wt. % corn-starch, where the reversible discharge capacity in the first cycle was about 100 $mAhg^{-1}$. That corresponds to the reversible extraction/insertion of 0.66 Li ions per formula unit assuming that the discharge capacity is solely due to Li insertion. Accordingly, it can be concluded that only the Mn^{3+}/Mn^{2+} redox couple is active in the materials within the voltage range of 1.5-4.5 V. Higher corn-starch contents result in a slight capacity decrease. This can be attributed to the fact that less active material per weight of a cathode is present. Interestingly, the behavior changes at higher charge rate (in this case C/4), and cathodes containing 35, 45, and 50 wt. % corn-starch showed an increase in rate capability and thus higher capacities compared to the sample made with 25 wt. % corn-starch. Converting these values to reversible Li exchange values, the sample containing 25 wt. % corn-starch showed only a reversible exchange of 0.2 Li per formula unit, while a sample with 50 wt. % corn-starch showed a reversible exchange of 0.43 Li per formula unit. This indicates that the electronic conductivity which is even more important at higher rates is improved due to the increased residual carbon content. In addition, the decreased particle size of samples with higher residual carbon content could enhance the kinetics of Li-extraction/insertion. Samples containing 45 and 50 wt. % corn-starch show very similar external surface areas and rate capabilities as shown in Fig. 5 a) and 7 b), respectively. Coin cells with cathodes containing 25 and 50 wt. % corn starch were also cycled up to 4.8 V. The charge and discharge was done with a charge rate of C/100 to investigate slow rate performance and at a charge rate of C/33 for 100 cycles for long-term performance investigations. Results are shown in Fig. 8. Here, the top abscissa in Fig. 8a and b shows the specific capacity per gram LMS (carbon content is subtracted from the mass of the composite to give active material mass) while the bottom abscissa shows the specific capacity per gram LMS/C composite. The slow cycling at

a charge rate of C/100 resulted in a reversible capacity of 155 $mAhg^{-1}$ and 140 $mAhg^{-1}$ in the first cycle for cathodes containing 25 wt. % and 50 wt. % corn-starch, respectively. The corresponding irreversible capacity loss in the first cycle was 40 and 38.5 %, indicating that more Li ions were extracted than inserted. Taking the carbon content of 9 and 27 wt. % into account and disregarding the minor impurities of both samples gives initial discharge capacities of 170 $mAhg^{-1}$and

192 $mAh\text{-}g^{1}$ respectively. The value of the sample containing 25 wt. % corn-starch corresponds well to the reversible extraction/insertion of one Li per formula and the 50 wt. % shows reversible Li exchange of 1.15 Li per formula unit under the same assumption as mentioned before. Furthermore, the sample containing 25 wt. % corn-starch shows an even more severe capacity fading already in the second cycle, where the discharge capacity already dropped by 11 % down to 138 $mAhg^{-1}$, while the 50 wt. % sample only showed a 4 % capacity drop. This might indicate that the amorphization of LMS shows a more prominent impact on the Li-extraction/insertion kinetics of larger particles present in the 25 wt. % corn-starch sample.

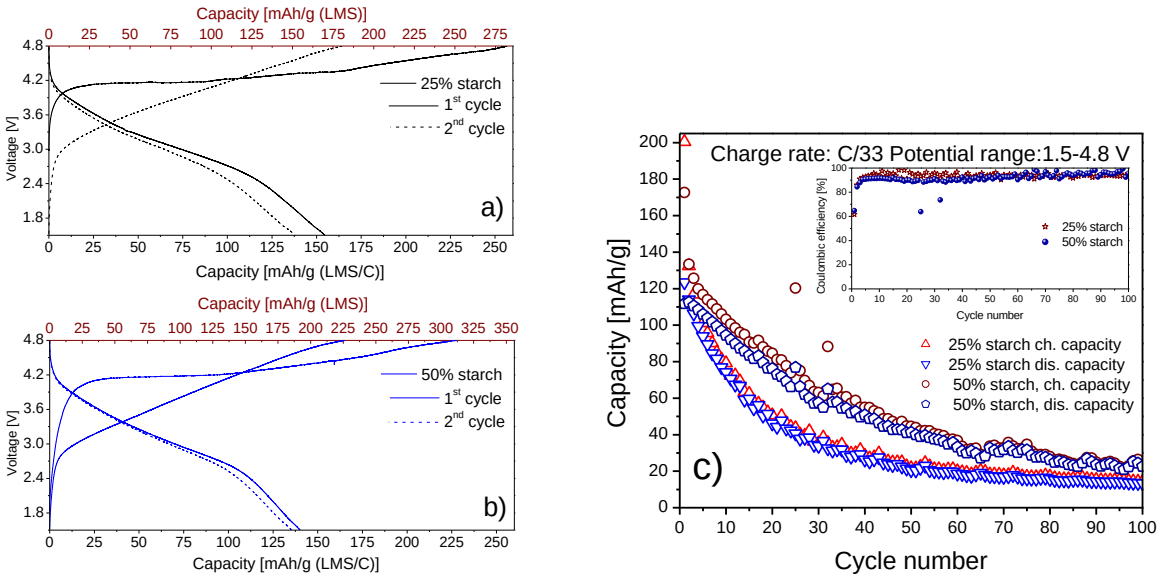

Fig. 8: First two galvanostatic cycles of LMS cathodes offering 25 % a) and 50 wt. % b) corn-starch as carbon source up to 4.8 V at C/100. Bottom abscissa shows specific capacity per g LMS/c composite, top abscissa the specific capacity per g LMS. c) 100 cycles of cathodes offering 25 % a) and 50 wt. % corn-starch at C/33

The same trend is visible in Fig. 8c. The sample containing 25 wt. % corn-starch shows more severe capacity fading on the first 20 cycles compared to the 50 wt. % one. The inset of Fig. 8 b shows the coulombic efficiency which exhibits values between 90 and 100 % for both samples after the first few cycles.

If it is assumed that the majority of the first charge capacity is due to Li extraction, then the irreversible capacity loss in the first cycle gives a direct indication of a partly collapsed structure that does not allow full re-lithiation during the following discharge. This effect is supposed to be more prominent the more Li is extracted [25]. Table 1 shows corrected (mass of carbon is subtracted) charge and discharge capacities and the irreversible capacity loss in percent of

cathodes synthesized using 25-50 wt. % corn-starch. Samples synthesized without or with a low amount of corn-starch addition are excluded because they showed very little or no electrochemical activity.

Table 2: Irreversible capacity loss and corrected capacities during the first cycle of samples cycled at C/33 between 1.5 and 4.5 V

Sample	Charge capacity 1st cycle [mAhg^{-1}(LMS)]	Discharge capacity 1st cycle [mAhg^{-1}(LMS)]	Irreversible capacity loss [%]
25 wt. % corn-starch	156.7	110.7	29.4
35 wt. % corn-starch	136.8	107.1	21.7
45 wt. % corn-starch	141.3	109.4	22.6
50 wt. % corn-starch	148.5	109.3	26.4

A trend of increasing irreversible capacity loss with increasing first charge capacity is visible indicating a higher degree of structural collapse when more Li is extracted. Furthermore, the charge plateau in the second cycle is in all cases shifted to lower potentials which would also indicate structural changes [26]. Recently, Devaraj *et al.* reported about LMS with a distinct charge and discharge plateau during the first ten cycles indicating a preserved structure before degradation occurred [13]. This behavior was neither observed here, nor in other studies [4-6, 8-12, 14-15]. Apart from the first charge, which shows a plateau at about 4.2 V no distinct charge plateaus were present. This also indicates structural degradation. The irreversible capacity is not solely due to structural collapse. In reality it is most probably a combination of irreversible electrolyte oxidation and structural degradation which becomes more prominent the more Li is extracted.

4 Conclusions

The successful preparation of porous nano-sized LMS/C by a PVA assisted sol-gel method is reported. The addition of corn-starch was shown to be crucial for phase purity during the carbothermal reduction step as well as for the electrochemical performance by building up a conductive coating around the particles. In addition, it seems to hinder particle growth to a certain extent so that the resulting powder offers a high amount of porosity in the meso/macro range and a huge increase in accessible surface area. Also the effect of the atmosphere and thus p_{o2} was shown to be of major importance for the synthesis of LMS. Highest phase purities of 95 % or higher were achieved when heat treatments were carried out in 5 % H_2 (H-Ar-mix-5) and starch contents were ≥ 25 wt. %. Samples synthesized under these conditions were indexed to the orthorhombic space group $Pmn2_1$ and showed only minor traces of secondary phases, namely MnO and Li_2SiO_3. If the applied corn-starch amount was 15 wt. % or lower, powders consisted of a mixture of orthorhombic $Pmn2_1$ and orthorhombic Pmnb polymorph of LMS in addition to an increased amount of secondary phases. The highest reversible capacity was observed using powder offering 25 wt. % corn-starch addition during synthesis. Coin-cells using this powder as cathode offered a discharge capacity of 155 $mAhg^{-1}$ cycled at C/100 and 124 $mAhg^{-1}$ cycled at C/33 in the first cycle. The first value corresponds approximately to the reversible extraction/insertion of one Li per formula unit taking the carbon content of the sample into consideration. Unfortunately all samples showed relatively low rate capabilities and irreversible capacity fading during cycling, which is believed to be the result of a partly collapsed (amorphous) structure during cycling [25].

Acknowledgements

The authors gratefully acknowledge the Research Council of Norway for funding of the SilicatBatt project (grant number: 216469/E20). NORTEM seed and competence projects (grant number 11) and Dr. Per Erik Vullum are acknowledged for TEM analysis. Dr. Julian Tolchard is acknowledged for assistance with Rietveld analysis and Prof. Thomas Jüstel for allowing use of the carbon determination facilities of Münster University of Applied Science Germany.

References

[1] Padhi, A. K., Nanjundaswamy, K. S., Goodenough, J. B. *Phospho-olivines as Positive-Electrode Materials for Rechargeable Lithium Batteries. J. Electrochem. Soc*, **1997,** 144, 1188-1194.

[2] Saiful Islam M., Dominko R., Masquelier C., Sirisopanaporn C., Armstrong A. R., Bruce P. G., *Silicate cathodes for lithium batteries: alternatives to phosphates?, J. Mater. Chem.,* **2011,** 21, 9811-9818.

[3] B. L. Ellis, K. T. Lee, L. F. Nazar, *Positive Electrode Materials for Li-Ion and Li-Batteries, Chem. Mater.* **2010,** 22, 691–714.

[4] Dominko R., Bele M., Gaberšček M., Meden A., Remškar M., Jamnik J., *Structure and electrochemical performance of Li_2MnSiO_4 and Li_2FeSiO_4 as potential Li-battery cathode materials, Electrochemistry Communications,* **2006,** 8, 217–222.

[5] Larsson P., Ahuja R., Liivat A., Thomas J. O., *Structural and electrochemical aspects of Mn substitution into Li2FeSiO4 from DFT calculations, Computational Materials Science* ,**2010,** 47 678–684.

[6] Dominko R., *Li_2MSiO_4 (M = Fe and/or Mn) cathode materials, Journal of Power Sources*, **2008,** 184, 2, 462-468.

[7] Gummow R. J., He Y., *Recent progress in the development of Li2MnSiO4 cathode materials, Journal of Power Sources*, **2014,** 253, 315-331.

[8] Li Y. X., Gong Z. L., Yang Y., *Synthesis and characterization of Li_2MnSiO_4/C nanocomposite cathode material for lithium ion batteries, J. Power Sources*, **2007**, 174, 528-532.

[9] Świętosławski M., Molenda M., Furczo K., Dziembaj R., *Nanocomposite C/Li_2MnSiO_4 cathode material for lithium ion batteries, Journal of Power Sources,* **2013,** 244, 510-514.

[10] Świętosławski M., Molenda M., Grabowska M., Wach A., Kuśtrowski P., Dziembaj R., *Electrochemical impedance spectroscopy study of C/Li_2MnSiO_4 composite cathode material at different states of charge*, *Solid State Ionics,* **2014,** 263, 99-102.

[11] Molenda M., Świętosławski M., Wach A., Majda D., Kuśtrowski P., Dziembaj R., *Stability of C/Li_2MnSiO_4 composite cathode material for Li-ion batteries towards $LiPF_6$ based electrolyte, Solid State Ionics,* **2014**, 262, 98-101.

[12] Sun, D., Wang H., Ping D., Zhou N., Huang X., Tan S., Tang Y., *In-situ synthesis of carbon coated Li_2MnSiO_4 nanoparticles with high rate performance, Journal of Power Sources*, **2013,** 242, 865-871.

[13] Devaraj S., Kuezma M., Ng C.T., Balaya P., *Sol-gel derived nanostructured Li2MnSiO4/C cathode with high storage capacity, Electrochimica Acta,* **2013,** 102, 290-298.

[14] Liu W. G., Xu Y. H., Yang R., *Synthesis and electrochemical properties of Li_2MnSiO_4/C nanoparticles via polyol process, Rare Metals,* **2010**, 29. 511-514.

[15] Aravindan V., Karthikeyan K., Kang K. S., Yoon W. S., Kim W. S., Lee Y. S., Influence of carbon towards improved lithium storage properties of Li_2MnSiO_4 cathodes, J. Mater. Chem., **2011**, 21, 2470–2475.

[16] Kojima A., Kojima T., Tabuchi M., Sakai T., *Synthesis of Li2MnSiO4 Cathode Material Using Molten Carbonate Flux Method with High Capacity and Initial Efficiency J. Electrochem. Soc.* **2012**, 159, A532-A537.

[17] Zhou H, Einarsrud M-A., Vullum-Bruer F., *High capacity nanostructured $Li_2Fe_xSiO_4$/C with Fe hyperstoichiometry for Li-ion batteries, Journal of Power Sources,* **2013,** 235, 234-242.

[18] Politaev V. V., Petrenko A. A., Nalbandyan V.B., Medvedev B. S., Shvetsova E. S., *Crystal structure, phase relations and electrochemical properties of monoclinic Li_2MnSiO_4, Journal of Solid State Chemistry,* **2007,** 180, 3, 1045-1050.

[19] Gummow R. J., Sharma N., Peterson V. K., He Y., *Crystal chemistry of the Pmnb polymorph of Li_2MnSiO_4, Journal of Solid State Chemistry,* **2012**, 188, 32-37.

[20] Duncan H., Kondamreddy A., Mercier P. H. J., Le Page Y., Abu-Lebdeh Y., Couillard M., Whitfield P. S., Davidson I. J., *Novel Pn Polymorph for Li_2MnSiO_4 and Its Electrochemical Activity As a Cathode Material in Li-Ion Batteries, Chem. Mater.*, **2011**, 23, 5446-5456.

[21] Zhou H, Einarsrud M-A., Vullum-Bruer F., *PVA-assisted combustion synthesis and characterization of porous nanocomposite Li_2FeSiO_4/C, Solid State Ionics,* **2012**, 225, 585-589.

[22] Brunauer S., Emmett P. H., Teller E., *Adsorption of Gases in Multimolecular Layers, Journal of the American Chemical Society,* **1938,** 60, 309-319.

[23] Harkins W. D., Jura G., *Surfaces of solids. XII. A vapor adsorption method for the determination of the area of a solid without the assumption of a molecular area, and areas occupied by nitrogen and other molecules on the* surface of a solid. *Journal of the American Chemical Society,* **1944,** 66 1366-1373.

[24] Barrett E. P., Joyner L. G., Halenda P. P., *The Determination of Pore Volume and Area Distributions in Porous Substances. I. Computations from Nitrogen Isotherms, Journal of the American Chemical Society,* **1951,** 73, 373-380.

[25] Dominko R., Bele M., Kokalj A., Gaberscek M., Jamnik J., *Li_2MnSiO_4 as a potential Li-battery cathode material, Journal of Power Sources,* **2007,** 174, 2, 457-461.

[26] Nytén A., Kamali S., Häggström L., Gustafsson T., Thomas J.O., *The lithium extraction/insertion mechanism in Li_2FeSiO_4, Journal of Materials Chemistry,* **2006,** 16 , 23, 2266-2272.

Figure captions

Fig 1: Summarizing flow chart with optimized parameters for the LMS and LMS/C synthesis

Fig. 2: a) Phase composition for different heat treatment atmospheres. b) Phase fraction for different starch contents at optimized synthesis parameters

Fig 3: a) Powder XRD pattern (CuK$_\alpha$ radiation) of LMS/C synthesized with optimized parameters and different corn-starch contents. Residual carbon content is given. Asterisk marks the unidentified secondary phase in the 5% sample. b) Full pattern refinement (MoK$_\alpha$ radiation) of a LMS/C sample

Fig 4: Carbon content of LMS/C samples heat treated in H-Ar-mix-5 and in Ar respectively

Fig. 5: a) BET surface area for powders with varying corn-starch content, including isotherms and micro-pore/external area separation. b) Pore size distribution for powders with varying corn-starch content

Fig. 6: TEM micrographs of a) the agglomerate structure of a sample containing 25 wt. % corn-starch, b) the carbon coating of a sample containing 25 wt. % corn-starch, c) the

porosity of the carbon coating of a sample containing 50 wt. % corn-starch and d) the electron diffraction pattern

Fig. 7: Galvanostatic cycling of LMS cathodes offering a varying amount of corn-starch as carbon source. a) First two cycles at C/33. b) Reversible discharge capacity for 15 cycles at different charge rates

Fig. 8: First two galvanostatic cycles of LMS cathodes offering 25 % a) and 50 wt. % b) corn-starch as carbon source up to 4.8 V at C/100. Bottom abscissa shows specific capacity per g LMS/c composite, top abscissa the specific capacity per g LMS. c) 100 cycles of cathodes offering 25 % a) and 50 wt. % corn-starch at C/33

Table captions:

Table 1: Heat treatment atmospheres and carbon source amount of samples A-D

Table 2: Irreversible capacity loss and corrected capacities during the first cycle of samples cycled at C/33 between 1.5 and 4.5 V

Supporting material captions

Fig. 1: Powder XRD pattern of dried gel aged for 72 h

Fig. 2: Powder XRD pattern of calcined LMS precursor

Fig. 3. HKL planes of $Pmn2_1$ Li_2MnSiO_4

Fig. 4: Pmnb polymorph, Mn_2SiO_4 and MnO secondary phases in LMS containing 5 wt. % corn-starch

Fig. 8: Galvanostatic cycling of LMS cathodes a) without corn-starch as carbon source b) with 5 wt. % corn-starch as carbon source